Pseudopotentials for non-local-density functionals

G. Ortiz
Institut Romand de Recherche Numérique en Physique des Matériaux (IRRMA), PHB-Ecublens, 1015 Lausanne, Switzerland

P. Ballone
Institut de Physique Expérimentale, Ecole Polytechnique Fédérale de Lausanne, PHB-Ecublens, 1015 Lausanne, Switzerland

(Received 22 October 1990)

Ab initio pseudopotentials for the IIA and IIB elements have been generated in the framework of density-functional theory, including gradient corrections to the local-density approximation (LDA). Their accuracy and transferability have been tested by extensive atomic computations. We applied these pseudopotentials to the evaluation of bonding properties of homonuclear dimers. Our molecular computations, not restricted to light elements, allow a wide assessment of the importance of gradient corrections in finite systems. For all the dimers considered here, the LDA error for bond energies is reduced by roughly 50%. The relative improvement on equilibrium distances and vibrational frequencies is less impressive, but still important and systematic. We discuss the computational cost for the evaluation of gradient corrections in computer programs based on the plane-wave (or plane-wave-like) basis-set expansion.

I. INTRODUCTION

Density-functional theory[1] (DFT) in the local-density approximation[2] (LDA) is the basic tool for most of the modern computational physics devoted to the understanding of electronic and structural properties of condensed matter. A large and growing body of computations within this scheme has assessed its ability to describe a variety of properties of real materials, and has also highlighted its limitations.[3,4]

Due to its fundamental and technological implications, the poor description by LDA (and, more generally, within DFT) of electronic excitations in semiconductors and insulators has been the main focus of theoretical investigation. Less discussed, but still very well known, are several other problems, among which are the following:

(i) Cohesive energies of condensed systems are systematically overestimated. The discrepancy between computed and measured quantities becomes more severe in going from solids to surfaces and to finite systems, like molecules and clusters.

(ii) Equilibrium interatomic distances are systematically underestimated. The relative error is usually quite small, but pathological cases are known, especially among finite systems. Typical examples are given by small aggregates of IIA and IIB elements, for which the error on the equilibrium distances may be as large as 10%. For these systems, the vibrational frequencies are largely overestimated, sometimes by as much as 50%.[5,6]

(iii) The stability of negatively charged finite systems is underestimated. In particular, LDA predicts negative electron affinities for experimentally stable ions like H^-, O^-, F^-, Ca^-, etc.

While the problem of optical excitations is outside the range of validity of DFT, the problems listed above concern ground-state properties, and, in principle, it should be possible to improve on LDA without giving away the many (conceptual and computational) advantages of DFT.

The importance of overcoming these limitations within a simple and viable computational scheme has recently been enhanced by the introduction of simulation methods[7] relying on the LDA Born-Oppenheimer energy surface to study the dynamics and thermal properties of complex systems.

In the last few years, a variety of recipes has been proposed to improve LDA within the DFT framework. While we refer to a recent review for a systematic discussion (see, for instance, Ref. 8 or Ref. 4), we would like to mention the self-interaction correction (SIC) of Perdew and Zunger;[9] the Hartree-Fock plus local correlation (LSDX) of Kohn and Sham (KS);[2] the average (AD) and weighted density (WD) of Gunnarson, Lundqvist, and collaborators;[10–13] and, finally, the gradient-corrected (GC) LDA developed by Perdew, Langreth, and Mehl.[14–17]

In our opinion, and especially in the perspective of including an improved exchange-correlation approximation in a total-energy molecular-dynamics algorithm, the GC LDA has several important advantages over the other schemes:

(i) It provides a unique potential for all the orbitals, with a clear practical and conceptual simplification.

(ii) It is computationally very convenient, especially for algorithms based on the plane-wave expansion, since the gradient and the Laplacian of the charge density, required by this scheme, are efficiently evaluated by fast Fourier transform.

Moreover, previous computations for atoms, molecules, and solids have shown that GD schemes are indeed

promising, at least for what concerns cohesive energies and structural properties. Stimulated by these positive features, several variants of the original Langreth-Mehl formulation have been proposed.[18–21] Despite their successes, GC LDA schemes have not replaced the LDA as the current approximation to the exchange-correlation functional in total-energy computations.

One of the reasons for this is that the improvement on LDA has been considered marginal, especially for the gap problem[22] or the description of Fermi surfaces for transition metals.[23] Another reason is probably the lack of some basic tools, like computer codes and pseudopotentials.

Although important, the first limitation should be used only with care to gauge the quality of approximations to the exact DFT. As already mentioned, band gaps are outside the reach of DFT, and also for the Fermi surface there is evidence that, in general, this is not correctly described by the k dependence of the (exact) highest occupied Kohn-Sham eigenvalue.[24]

To ease the second problem, in the present paper we compute and compare pseudopotentials generated within different GC schemes. In doing this, we concentrate on the IIA and IIB elements, for which LDA provides poor cohesive energies and equilibrium geometries, especially in the case of small aggregates.

These pseudopotentials are accurately tested for transferability and applied to the computation of bonding properties of homonuclear dimers. Our results confirm that GC approximations provide a systematic and substantial improvement on LDA for the computation of potential-energy surfaces.

Among the different GC schemes, the exchange formula by Becke[21] and the correlation energy by Perdew[19] hold the greatest promise for a reliable description of both the finite and the extended systems, together with the ability to provide smooth and transferable pseudopotentials.

The layout of the paper is as follows: In Sec. II we briefly review the gradient-corrected LDA schemes. In Sec. III we present the results of all-electron atomic computations and we discuss the comparison with other schemes and, in particular, with the SIC. The generation of pseudopotentials is described in Sec. IV, where we also report the results of the transferability tests. In Sec. V we present the results of the computation of bonding properties for the neutral, homonuclear dimers of the IIA and IIB elements and we discuss the computational cost for the evaluation of the exchange and correlation functional in algorithms based on the plane-wave expansion. Final remarks and an outline of future work are contained in the Sec. VI. While completing the present paper, we became aware of a study by Shirley *et al.*[25] in which nonlocal-exchange-correlation functionals (LSDX and LDA SIC) are applied to the generation of *ab initio* pseudopotentials.

II. GRADIENT CORRECTIONS TO THE LDA

Following the basic results of DFT,[1,2] we express the ground-state energy of N electrons in the external potential $\hat{V}_{\text{ext}}$ as (atomic Hartree units are used throughout the paper)

$$E[\rho]=\sum_i f_i\langle\psi_i|-\tfrac{1}{2}\nabla_i^2+\tfrac{1}{2}V_H+\hat{V}_{\text{ext}}|\psi_i\rangle+E_{\text{XC}}[\rho]\ , \quad (1)$$

where ρ is the electron density

$$\rho(\mathbf{r})=\sum_i f_i|\psi_i(\mathbf{r})|^2 \quad (2)$$

and the sums extend over the occupied independent particle orbitals $\{\psi_i\}$ whose occupation numbers are f_i. In Eq. (1), V_H is the Hartree potential

$$V_H(\mathbf{r})=\int\frac{\rho(\mathbf{r}')d\mathbf{r}'}{|\mathbf{r}-\mathbf{r}'|} \quad (3)$$

and $E_{\text{XC}}[\rho]$ is the exchange-correlation (XC) energy functional.

As is well known, the basic approximation of LDA consists in writing $E_{\text{XC}}[\rho]$ for an inhomogeneous system as

$$E_{\text{XC}}^{\text{LDA}}[\rho]=\int\rho(\mathbf{r})\varepsilon_{\text{XC}}(\rho(\mathbf{r}))d\mathbf{r}\ , \quad (4)$$

where ε_{XC} is the exchange-correlation energy per particle of a uniform electron gas, evaluated at the local density $\rho(\mathbf{r})$.

The simplest possibility of adding some more information on the density distribution is via the inclusion of the gradients of $\rho(\mathbf{r})$ in the XC functional. Then symmetry and dimensional arguments determine the form of the first correction to $E_{\text{XC}}^{\text{LDA}}$ in a Taylor-like functional expansion for $E_{\text{XC}}[\rho]$ to be[26]

$$E_{\text{XC}}^{\text{GC}}=E_{\text{XC}}^{\text{LDA}}+C\int\frac{|\nabla\rho(\mathbf{r})|^2}{\rho(\mathbf{r})^{4/3}}d\mathbf{r}\ , \quad (5)$$

where C is a constant determined by the response functions of the homogeneous electron gas.

Early computations for the planar, metallic surface,[27,28] however, made it clear that, far from providing an improvement, Eq. (5) was, in fact, giving worse results than LDA for both the surface energy and the density profile. The analysis of this failure by Gunnarsson, Lundqvist, and collaborators,[10] carried out in terms of the size and shape of the exchange-correlation hole, evolved in the weighted-density approximation.[11–13]

Following a different line of investigation, Langreth, Perdew, Mehl, and co-workers concentrated on the Fourier-space analysis of the exchange-correlation functional.[14–16] Expressing the XC energy as

$$E_{\text{XC}}=\frac{1}{2\pi^2}\int_0^\infty E_{\text{XC}}(k)k^2dk \quad (6)$$

and starting again from the case of the planar jellium surface, they were able to show that LDA provides the exact limit of $E_{\text{XC}}(k)$ for large k vectors. On the other hand, they obtained the exact low-k limit of $E_{\text{XC}}(k)$ within the random-phase approximation (RPA). Interpolating between these two limits, they proposed the following expression for E_{XC} [referred to as the Langreth and Mehl (LM) approximation in the following] in terms of the density ρ and its gradient:

$$E_{\rm XC}^{\rm LM}=E_{\rm XC}^{\rm LDA}({\rm RPA})+a\int\frac{|\nabla\rho(\mathbf{r})|^2}{\rho(\mathbf{r})^{4/3}}(2e^{-F}-\tfrac{7}{9})d\mathbf{r}\ , \tag{7}$$

where

$$F=b\frac{|\nabla\rho(\mathbf{r})|}{\rho(\mathbf{r})^{7/6}}\ . \tag{8}$$

The constant a is atomic Hartree units is

$$a=\frac{\pi}{16(3\pi^2)^{4/3}} \tag{9}$$

and b is an adjustable parameter introduced in order to join smoothly the two (LDA and RPA) limiting approximations. The value suggested by Langreth and Mehl was $b=(9\pi)^{1/6}f$ with $f\sim 0.15$. Refinements for finite[16] and spin-polarized[17] systems have also been proposed. It is important to note that the specific interpolation form and the value of the b parameter depend on the choice of RPA to describe the local contribution $E_{\rm XC}^{\rm LDA}$.

Though appealing and, in many respects, successful, the LM exchange-correlation energy has several drawbacks. The most serious one, first discussed by Perdew,[19] is that in the limit of homogeneous systems $E_{\rm XC}^{\rm LM}$ approaches the RPA XC energy for the uniform electron gas, instead of recovering the exact result, as computed, for instance, by quantum Monte Carlo methods.[29] As emphasized in Ref. 19, this may not be too serious for atoms or molecules, but it is indeed an important limitation for the description of the valence charge in many solids (like simple metals). Another drawback, common to most of the gradient-corrected schemes, concerns the asymptotic behavior of the XC potential close to the atomic nucleus, and, for finite systems, in the tail of the electron distribution (see Ref. 16 and the discussion below).

To overcome these and other related problems, the XC energy was split into its exchange and correlation contribution. For the exchange part, Perdew and Wang (PW) (Ref. 18) proposed a gradient expansion based on the analysis of the behavior of the exchange hole in inhomogeneous systems. For the correlation part, an interpolation formula was proposed,[19] based on the electron-gas results of Hu and Langreth[30] and Rasolt and Geldart.[31] We shall refer to the combined XC functional as the PW approximation.

This scheme was shown to provide very good results for the exchange energy of atoms. However, as we shall discuss in detail in Sec. II, the satisfactory performance of the exchange energy is partly due to the compensation of errors in different regions of the charge distribution. Far from the nucleus of neutral atoms, the PW potential fails to reproduce the correct $-1/r$ behavior of the exchange potential.[32] Instead, as can easily be shown by assuming an exponentially vanishing density, it tends exponentially to zero as $\rho^{1/5}$. Close to the nucleus, the PW gradient contribution diverges as $-\alpha/r$ (where α is a constant), thus overcorrecting the LDA behavior.

The need to limit the gradient corrections in regions of high gradient [large ratio $|\nabla\rho(\mathbf{r})|/\rho^{4/3}(\mathbf{r})$] and to recover the correct asymptotic behavior of the exchange potential in the tail of the charge distribution was emphasized by Becke in Ref. 20 and 21.

On semiempirical grounds, he proposed the following interpolation for the exchange energy:

$$E_X^B=E_X^{\rm LSD}+\sum_{\sigma=\pm}\int f(\rho_\sigma;\nabla\rho_\sigma)d\mathbf{r}\ , \tag{10}$$

where

$$f(\rho_\sigma;\nabla\rho_\sigma)=-\beta\rho_\sigma^{4/3}\frac{x_\sigma^2}{(1+6\beta x_\sigma\sinh^{-1}x_\sigma)}\ , \tag{11}$$

with $x_\sigma=|\nabla\rho_\sigma|/\rho_\sigma^{4/3}$, and $\beta=0.0042$ a.u. is determined by a fit to atomic Hartree-Fock data. The sum is over the two spin components $\sigma=\pm 1$. The exchange potential corresponding to Eq. (10), straightforward but tedious to compute, is reported in Appendix A.

By assuming an exponentially decaying asymptotic density, it is easy to verify that, far from atoms or molecules, the *exchange energy per particle* tends to the limit

$$\lim_{r\to\infty}\varepsilon(r)=-1/r\ . \tag{12}$$

It does not, however, provide the correct asymptotic behavior for the exchange *potential*.[32] From Eq. (A2) of Appendix A, instead, it is apparent that $v_x^B(r)\sim -1/r^2$ in the exponential tail of the density distribution. One could argue that this asymptotic form is still a definite improvement on the LDA behavior, with $v_x^{\rm LDA}$ vanishing exponentially with r, or on the LM asymptotic positive divergence of $v_x^{\rm LM}(r)$. However, v_x^B attains its asymptotic region so far away in the density tail as to have a negligible effect on the computed quantities. In the intermediate region, where the negative, slowly decaying part of the exchange potential is expected to be important for the determination of excitation, ionization energies, and electron affinities, the gradient term in v_x^B is small, positive, and close to the PW exchange correction. Again, we conclude that the very good exchange and total energies obtained for atoms are partly due to compensation of errors in the core and in the tail of the electron distribution. In the following sections we shall implement the Becke approximation for the exchange energy together with the Perdew formula[19] for correlation (BP approximation).

Out of the several gradient-corrected schemes proposed in the literature, the LM formula has been the most extensively tested. During the years since its appearance, it has been applied to atoms,[33] molecules,[34] and extended solids.[35] Recently it has been used for an improved analysis of the jellium surface.[36]

In all these tests, the LM formula gave encouraging results, at least for what concerns ground-state properties like total and cohesive energies, ionization energies, density distributions, and equilibrium geometries. As mentioned in the Introduction, it failed to improve significantly the band structure of silicon[22] and of some transition metals.[23] In the following sections we compare the three recipes listed above in atomic computations, and we test their ability to produce pseudopotentials with the desirable characteristics of smoothness and transferability.

TABLE I. Atomic total energies (in Hartrees) for the IIA and IIB elements computed in LDA and the gradient-corrected schemes discussed in the text. The last entry reports the experimental value for Be, Mg, and Ca (Ref. 38) and the relativistic Hartree-Fock energy (numbers in parentheses) for the heavier elements (Ref. 39).

Element	LDA	LM	PW	BP	Expt.
Be	14.448	14.609	14.685	14.661	14.676
Mg	199.446	200.015	200.512	200.412	200.418
Ca	678.672	679.725	680.747	680.603	680.472
Sr	3175.783	3177.976	3180.180	3180.223	(3178.127)
Ba	8129.246	8132.828	8136.398	8136.818	(8136.053)
Zn	1793.294	1794.952	1796.606	1796.537	(1794.628)
Cd	5589.566	5592.513	5595.414	5595.666	(5593.480)
Hg	19 611.740	19 617.631	19 623.444	19 624.699	(19 653.870)

III. ALL-ELECTRON ATOMIC COMPUTATIONS

The three XC functionals described above have already been used by several groups in nonrelativistic computations for light atoms. Here we extend these tests to the heavy elements by performing scalar relativistic all-electron computations for all the elements of the IIA and IIB groups. For the local part of the XC energy we used the Vosko-Wilk-Nusair[37] parametrization, both for the RPA approximation (entering the LM approximation) and for the interpolation to the "exact" uniform electron-gas data.[29]

In Table I we compare the total energies of the IIA and IIB atoms computed in the various schemes. The values provided by the gradient-corrected formulas are all significantly lower than those of LDA. For Be, Mg, and Ca, the BP approximation is indeed very close to the experimental result.[38] For heavier elements no reliable experimental value is available, and in the table we compare to relativistic Hartree-Fock (HF) computations.[39] Through all the series the energy ordering is the same:

$$E_{\rm tot}^{\rm PW} \sim E_{\rm tot}^{\rm BP} < E_{\rm tot}^{\rm LM} < E_{\rm tot}^{\rm LDA} \tag{13}$$

and $E_{\rm tot}^{\rm BP}$ tends to be slightly lower in energy than either the experimental value or the HF result (Be and Hg being the only two exceptions).

In contrast with total energies, the first ionization potentials of all the elements considered here are accurately known from experiment. In Tables II and III we compare the predictions of LDA and the gradient-corrected approximations to the measured values for the first ionization potential (IP1) and for the removal energy (RE) of the valence shell—equal, for these elements, to the sum of the first and second ionization energies. The theoretical values are computed as energy differences between the ionized and neutral ground states. The energy of the singly ionized atoms is computed within the spin-density version of each functional. As is well known, LDA is al-

TABLE II. First ionization potential (in eV) for the IIA and IIB elements computed in LDA and in the gradient-corrected schemes. The results of pseudopotential computations are reported in parentheses (LDA pseudopotentials are from Ref. 45; for the GC schemes we applied our fitted pseudopotentials).

Element	LDA	LM	PW	BP	Expt.
Be	9.027	9.081	9.240	9.095	9.322
	(8.969)	(9.239)		(9.070)	
Mg	7.733	7.608	7.940	7.700	7.646
	(7.631)	(7.824)		(7.645)	
Ca	6.236	6.133	6.412	6.188	6.113
	(6.137)	(6.301)		(6.128)	
Sr	5.867	5.764	6.031	5.807	5.695
	(5.761)	(5.950)		(5.729)	
Ba	5.379	5.294	5.529	5.319	5.212
	(5.271)	(5.458)		(5.265)	
Zn	9.913	9.670	10.067	9.736	9.394
Cd	9.414	9.143	9.455	9.193	8.993
	(9.411)	(9.152)		(9.208)	
Hg	10.865	10.672	10.800	10.631	10.437
	(10.819)	(10.701)		(10.655)	

TABLE III. Valence-shell removal energies (first and second ionization potential) in eV for the IIA and IIB elements computed in LDA and in the gradient-corrected schemes. The results of pseudopotential computations are reported in parentheses.

Element	LDA	LM	PW	PB	Expt.
Be	27.284	27.438	27.768	27.489	27.534
	(29.029)	(27.713)		(27.421)	
Mg	23.109	22.750	23.481	22.985	22.681
	(22.694)	(23.150)		(22.829)	
Ca	18.401	18.077	18.698	18.244	17.985
	(17.964)	(18.347)		(18.028)	
Sr	17.232	16.913	17.498	17.053	16.726
	(16.762)	(17.166)		(16.821)	
Ba	15.703	15.438	15.944	15.533	15.216
	(15.225)	(15.665)		(15.291)	
Zn	28.948	28.436	29.209	28.598	27.358
Cd	27.138	26.583	27.133	26.688	25.902
	(27.098)	(26.635)		(26.708)	
Hg	30.433	30.071	30.228	29.985	29.194
	(30.298)	(30.162)		(30.025)	

ready able to reproduce the experimental values reasonably well, the average relative error being 3.4% for IP1 and 3.3% for the RE.

With the exception of the Perdew-Wang formula, gradient-corrected schemes systematically improve over these results. The best agreement with experiment is achieved by the LM formula (ΔIP1$=1.6\%$, ΔRE $=1.7\%$). Slightly worse than LM, but still significantly better than LDA, is the BP scheme.

Excitation energies from the atomic or ionic ground state to the lowest-lying configurations of P and D symmetry are also accurately known from experiment. To avoid the complications arising from the multiplet structures,[40] we concentrate on the singly charged ions, for which the ground and low-lying excited states are given by an electron or a hole around a closed shell. To remain within the reach of DFT, we restrict ourselves to the transitions from the ^2S ionic ground state to the states of lowest energy of ^2P and ^2D symmetry and compute the excitation energies as total-energy differences. The computed and measured values for Ca^+ and Cd^+ are compared in Table IV, the results for these two elements being representative of those obtained for the others. The PW and BP recipes show a slightly better agreement with experiment than LDA. However, it is apparent that the improvement is not systematic and quantitatively not important.

As is well known, in DFT there is no equivalent of the Koopman's theorem valid for Hartree Fock, and, in general, Kohn-Sham eigenvalues should not be interpreted as single-particle excitations. The exception to this rule is represented by the eigenvalue of the uppermost occupied orbital that, even in finite systems, corresponds in the exact DFT to the ionization potential.[32] In this respect, the deficiencies of LDA are well documented, the eigenvalue of the highest occupied orbital in atoms being equal to about 60% of the LDA ionization potential evaluated as the difference of ground-state energies. This inconsistency is only marginally reduced by the gradient-corrected schemes. Although this failure to improve the value of the highest eigenvalue is a rather complex issue, a possible explanation is offered by the analysis of the atomic

TABLE IV. Excitation energies (in eV) to the lowest energy state of P and D symmetry for Ca^+ and Cd^+. The results of pseudopotential computations are reported in parentheses.

Transition	LDA	LM	Ca^+ PW	BP	Expt.
$^2S\rightarrow{}^2P$	3.155	3.035	3.179	3.104	3.144
	(3.068)	(3.214)		(3.052)	
$^2S\rightarrow{}^2D$	1.393	1.380	1.550	1.444	1.697
	(0.653)	(1.427)		(1.459)	
			Cd^+		
$^2S\rightarrow{}^2P$	5.919	5.936	5.795	5.868	5.703
	(5.864)	(5.917)		(5.841)	
$^2S\rightarrow{}^2D$	8.569	8.963	8.421	8.718	8.849
	(8.328)	(8.823)		(8.548)	

potential and charge distribution. Due to the strongly attractive gradient correction close to the nucleus, the core states of s symmetry are significantly lowered in energy and reduced in size with respect to their LDA counterparts. This results in a more effective screening of the nuclear charge and a stronger orthogonalization repulsion able to balance the gain in XC potential and to maintain the valence s states at an energy only slightly lower than the LDA value.

A few years ago Perdew and Zunger[9] discussed the limitations of the LDA in terms of the orbital self-interaction. In HF or exact DFT, the Hartree self-interaction apparently present in Eq. (1) is exactly cancelled by its exchange-correlation counterpart. This does not necessarily happen within approximations to the exact XC functional, like LDA or the gradient-corrected schemes. Furthermore, Perdew[41] proved that the relation

$$E_H^{\mathrm{SI}}[\rho]+E_{\mathrm{XC}}^{\mathrm{DF}}[\rho]=0 \tag{14}$$

is an exact one *for one-electron systems,* regardless of whether ρ is the ground-state density or not. In Eq. (14), E_H^{SI} is the Hartree self-interaction and $E_{\mathrm{XC}}^{\mathrm{DF}}$ is the exact XC energy of the spin-polarized density distribution $\rho(\mathbf{r})$.

On this basis, Perdew and Zunger proposed using

$$E^{\mathrm{SI}}=\sum_i f_i(E_H^{\mathrm{SI}}[\rho_i]+E_{\mathrm{XC}}^{\mathrm{appr}}[\rho_i]) \tag{15}$$

as a measure of self-interaction in the DF approximation specified by $E_{\mathrm{XC}}^{\mathrm{appr}}$ and to derive from this an improved functional $\tilde{E}_{\mathrm{XC}}^{\mathrm{appr}}$ by imposing, orbital by orbital, the relation

$$E_H^{\mathrm{SI}}[\rho_i]+\tilde{E}_{\mathrm{XC}}^{\mathrm{appr}}[\rho_i]=0\ . \tag{16}$$

The results for E^{SI} computed within different approximations for E_{XC} according to the definition of Eq. (15) are listed in Table V. If Eq. (15) is a faithful indicator of the quality of a DFT approximation, then the gradient-corrected schemes appear to be a major improvement on LDA.[42] However, we would like to mention that the interpretation of E^{SI} from Eq. (15) as self-interaction energy has some limitations. In fact, while the Hartree part is always defined without any ambiguity, for a many-electron system the identification of $E_{\mathrm{XC}}[\rho_i]$ as XC self-interaction of one orbital in the environment of all the others is much less evident.

An interesting feature of the gradient-corrected approximations is brought out by our numerical computations for atoms. Among the KS orbitals of a many-electron atom, some (i.e., the $1s$, $2p$, $3d$ $4f$) may be thought as the ground state (for a given symmetry) of a one-electron system in an external potential. For the others, having radial nodal surfaces, this is not possible. It is interesting to note that, within gradient-corrected schemes, orbitals of the first class contribute very little to E^{SI} [i.e., the exact relation (14) is only weakly violated], while the seconds are responsible for most of the residual self-interaction. This is in contrast to what is observed in LDA, where the inner-core states are the most affected by self-interaction that is, in fact, mainly a measure of localization. This may suggest that the gradient-corrected recipes discussed here are good approximations to the exact functional (at least for one-electron systems) only for density close to the ground-state density, while their density becomes rapidly worse moving away from the extremal point.

TABLE V. Self-interaction energies (in eV) of the ground-state atomic configuration computed in LDA and the GC schemes according to the definition of Perdew and Zunger (Ref. 9).

Element	LDA	LM	PW	BP
Be	6.682	0.750	−0.670	−0.321
Mg	38.039	7.417	−2.128	−1.193
Ca	78.088	7.504	−10.972	−11.506
Sr	201.456	11.952	−37.289	−42.060
Ba	340.721	−25.724	−105.574	−122.985
Zn	143.208	16.287	−21.126	−22.050
Cd	278.437	−0.704	−68.226	−78.356
Hg	582.266	−70.974	−221.092	−253.263

As a final point of this section, we display in Fig. 1 the XC potential for Sr computed in the various approximations discussed here. As mentioned in Sec. II, close to the nucleus the gradient-corrected exchange potentials diverge as $-\alpha/r$. In the intermediate region ($r<4$ a.u.) the exchange gradient-correction terms tend to be positive and present a characteristic shoulder around $r=1$ a.u. At large distances the LDA and PW curves vanish exponentially, while the LM potential diverges, taking positive values. Only for $r>10$ a.u. does the Becke potential attain its asymptotic behavior $v_x^B\sim -1/r^2$. Up to that point, the PW and Becke exchange potentials are re-

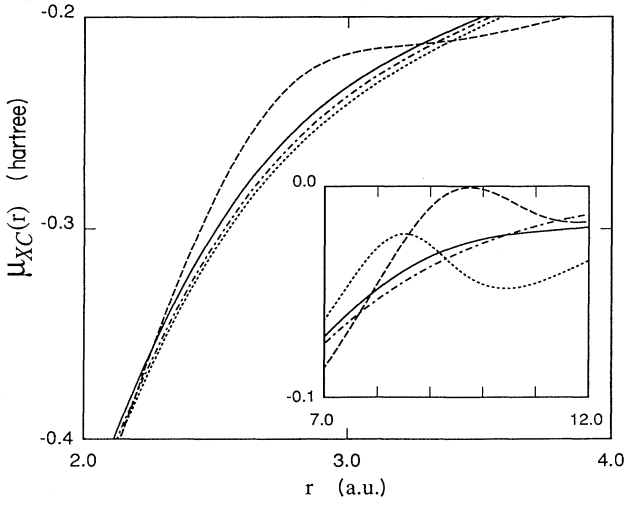

FIG. 1. Exchange-correlation potential μ_{XC} as a function of radial distance for a strontium atom. Dashed-dotted line, LDA; dashed line, LM; dotted line, PW; solid line, BP approximation.

markably similar. The addition of the correlation part tends to reduce the difference between LDA and GC schemes that, however, remains important in the range 2 a.u. $\leq r \leq 4$ a.u. and in the tail of the electron density.

IV. THE PSEUDOPOTENTIAL GENERATION

The atomic computations described above are the starting point for the construction of pseudopotentials to be used with the gradient-corrected XC formulas. In doing this, we followed closely the prescription given by Hamann in Ref. 43. For all the IIA elements we assumed a valence configuration given by the ns^2 electrons, where n is the principal quantum number of the highest occupied atomic level. For Cd and Hg we included in the valence the 12 electrons in the $(n-1)d^{10}ns^2$ levels. We did not produce any pseudopotential for Zn since the sharpness of its d component makes it of little use, at least for plane-wave programs.

In Fig. 2 we compare the $l=0$ component of the pseudopotential for Ca computed within the LDA, LM, and BP approximations. This plot is representative of the results obtained for the other elements.[44] The three pseudopotentials look quite similar, the main differences being confined to the region $r<1$ a.u., not really important for the computation of matrix elements since it is weighted by the r^2dr volume element. Less evident, but computationally more important, are the differences around the minimum of the pseudopotential, where the LM and BP curves are slightly shallower than the LDA result.

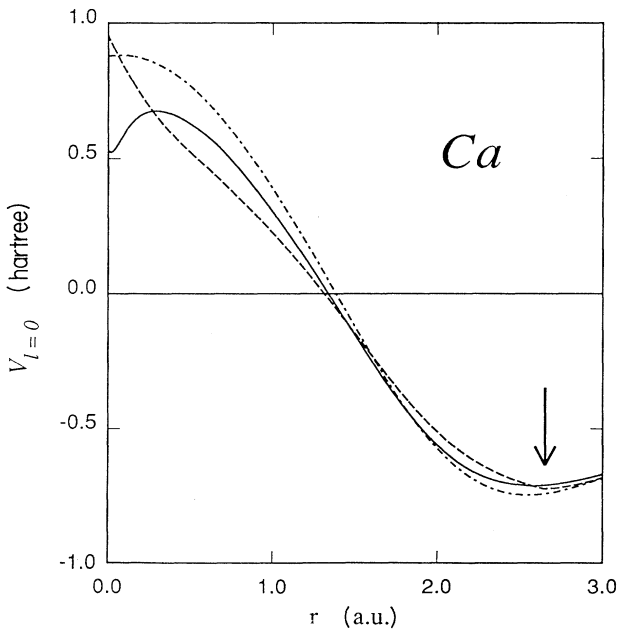

FIG. 2. $l=0$ component of the pseudopotential for Ca computed in LDA (dashed-dotted line, Ref. 45), LM (dashed line), and BP (solid line) approximations. The arrow indicates the position of a cusp in the LM pseudopotential.

The LM pseudopotential for Ca presents two cusps, at the origin and at $r=2.65$ a.u. (not evident on the scale of the figure). These singularities arise from the terms linear in $|\nabla\rho|$ present in the LM potential and giving a cusp wherever the pseudocharge density is stationary ($|\nabla\rho|=0$). The influence of these two singularities, however, is negligible, and they are removed in the process of fitting an analytic expression to the pseudopotential without significant changes in the computed properties of the pseudoatom (see below).

From a similar plot it is apparent that, despite the good quality of the all-electron atomic results, the PW scheme is not suitable to provide a smooth and regular pseudopotential. In fact, the pseudopotentials generated within this scheme have strange and funny shapes, with oscillations and other strong irregularities inside the core. Remembering the similarity of the total potential generated by the gradient-corrected schemes inside the core region (see Fig. 1), the pathological shape of the PW pseudopotential is quite surprising. To trace the origin of this behavior, we recall that the generation of the pseudopotential proceeds in several steps. First of all, a smooth pseudocharge density and screened potential are generated following, for instance, the recipe of Ref. 45. Then this potential is unscreened to compute the bare pseudopotential. It is mainly in this last step that differences arise among the gradient-corrected schemes, due to the significant differences in their exchange-correlation potentials for the relatively low densities and high gradients [large ratio $|\nabla\rho(\mathbf{r})|/\rho^{4/3}(\mathbf{r})$] characterizing the valence charge.

In an alternative scheme,[46] some information on the shape of the core charge density is retained in the computation of pseudopotentials in order to improve their transferability by taking into account the nonlinear exchange-correlation interaction between the core and valence charge. Following this prescription, the XC energy and potential of the pseudized system are computed for the sum of the valence and (smoothed) core charge, thus reducing the region of low density and high gradient to the tail of the charge distribution. As expected, this scheme reduces the differences among the gradient-corrected formulas and produces for all of them (including the PW) smooth and regular pseudopotentials. However, the inclusion of these nonlinear core corrections increases significantly the complexity of the computation. For this reason, in what follows we limit our analysis to the usual (linearized) pseudopotentials and to the gradient-corrected schemes (LM and BP) providing good results already at this level of approximation.

To make possible their publication in a compact form, we fitted the pseudopotentials (computed numerically on a logarithmic mesh) to a small set of analytic functions, following Ref. 45 both for the choice of the basis set and for the fitting procedure (see Appendix B below). In this process the loss of accuracy is insignificant. We verified that the difference in the ground-state atomic properties computed with the numerical or the fitted BP pseudopotential is, at most, 0.02 and 0.05 eV, respectively, for the eigenvalues and the total energies of the IIA elements

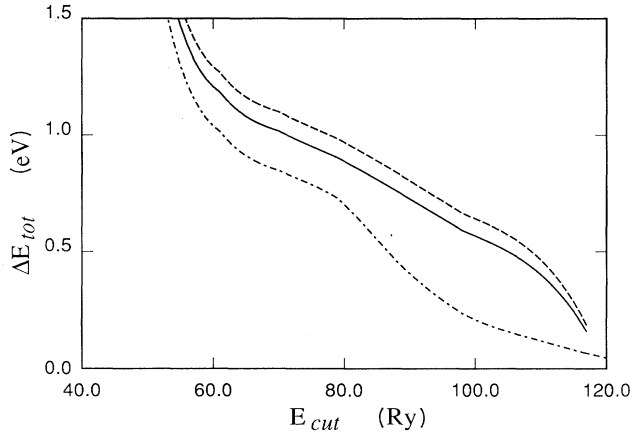

FIG. 3. Convergence of the total energy $E_{\rm tot}$ of a cadmium atom as a function of the kinetic-energy cutoff in LDA (dashed-dotted line), LM (dashed line), and BP (solid line) approximations. The asymptotic values $E_{\rm tot}(\infty)$ are provided by an atomic computation in spherical geometry on a logarithmic mesh.

and 0.07 and 0.2 eV for the IIB elements. For the LM pseudopotentials the error introduced by the fit is about two times larger than in the BP case.

As a first test of transferability, we computed the excitation and ionization energies of the pseudoatoms. These are compared to the results of the all-electron computation in Tables II through IV. From these data it appears that the transferability of the LM pseudopotentials is slightly worse than for the LDA ones. The performances of the BP pseudopotentials are more satisfactory, and, in fact, they are at least as good as those of the LDA pseudopotentials.

As a further test of the quality of the pseudopotentials, we have compared their convergence properties in a plane-wave expansion. As shown in Fig. 3 for cadmium, both the LM and BP pseudopotentials require a higher cutoff to achieve the same convergence in total energy obtained for the LDA. The cutoff increase, however, is not dramatic and does not prevent the use of gradient-corrected pseudopotentials in algorithms based on the plane-wave basis set.

V. BONDING PROPERTIES OF DIMERS

To test the ability of the gradient-corrected schemes, together with our pseudopotentials, to describe the Born-Oppenheimer surface of condensed systems, we computed the bonding parameters of homonuclear dimers of the IIA and IIB elements.[47]

As mentioned in the Introduction, these systems provide a severe test for theoretical methods, since they are characterized by weak cohesive energies, large equilibrium separations, and low vibrational frequencies. The description of their potential-energy curves, therefore, requires a precise cancellation of large attractive and repulsive contributions in the total energy. For instance, LDA substantially overestimate the cohesion, while Hartree-Fock gives monotonically repulsive curves. Moreover, small aggregates of these elements are the subject of several recent studies[48] that debate the possibility (experimentally confirmed for mercury clusters[49]) of an insulator-to-metal transition as a function of cluster size.

The algorithm we use for this computation has been described in a previous publication.[6] It is based on an expansion of the Kohn-Sham orbitals $\{\psi_i(\mathbf{r})\}$ in a basis of cylindrical waves adapted to the symmetry of the Hamiltonian,

$$\psi_i(\mathbf{r})=e^{\pm im\phi}\sum_{G_r}\sum_{G_z}C_i(G_r,G_z)e^{iG_z z}J_m(G_r r)\ . \tag{17}$$

Here we have introduced cylindrical coordinates (r,z,ϕ), with the z axis coincident with the symmetry axis of the dimer. m is the azimuthal quantum number; J_m is the Bessel function of the first kind and order m; G_r, and G_z are wave vectors selected by the boundary conditions (see Ref. 6 for more details). Despite the appearance of the Bessel functions, this basis set retains many of the properties and advantages of the plane-wave basis. In particular, it is orthogonal and its degree of completeness may be characterized by the single parameter $E_{\rm cut}$ (with the dimensions of an energy) specifying the kinetic-energy cutoff for the basis functions included in the computation

$$\tfrac{1}{2}(G_r^2+G_z^2)<E_{\rm cut}\ . \tag{18}$$

Furthermore, the computation of the gradient and the second derivatives of the density, required for the evaluation of the XC energy and potential, may be efficiently performed via a Fourier-Bessel transform (FBT). For instance, when the density is written as

$$\rho(\mathbf{r})=\sum_{G_r}\sum_{G_z}\tilde{\rho}(G_r,G_z)e^{iG_z z}J_0(G_r r)\ , \tag{19}$$

the gradient is given by

$$\frac{\partial\rho(\mathbf{r})}{\partial r}=-\sum_{G_r}\sum_{G_z}G_r\tilde{\rho}(G_r,G_z)e^{iG_z z}J_1(G_r r)\ , \tag{20}$$

$$\frac{\partial\rho(\mathbf{r})}{\partial z}=i\sum_{G_r}\sum_{G_z}G_z\tilde{\rho}(G_r,G_z)e^{iG_z z}J_0(G_r r)\ . \tag{21}$$

Taking into account the second derivatives ($\partial^2\rho/\partial r^2$, $\partial^2\rho/\partial r\partial z$, $\partial^2\rho/\partial z^2$), at each iteration of the minimization process it is necessary to compute five FBT's more than in the LDA case. Since the total number of FBT's per iteration required by the LDA scheme is $(2N+2)$ (see Ref. 6, Fig. 2), where N is the number of occupied orbitals, the relative importance of the gradient evaluation decreases rapidly with increasing the number of electrons in the system. For small molecules (like the IIA dimers), the additional five FBT's represent a sizable portion of the computation, which, however, remains reasonably small and fast.

In a three-dimensional plane-wave computation, nine additional Fourier transforms are needed to evaluate the gradient corrections to the energy and the potential.

TABLE VI. Bonding parameters for the homonuclear dimers of the IIA elements computed in LDA and in the GC schemes. r_e, D_e, and ω_e are the equilibrium distance, the cohesive energy, and the vibrational frequency, respectively. β, a, and b are the fitting parameters of the Hulburt and Hirshfelder formula [Eq. (22)].

Dimer (E_{cutoff})		r_e (a.u.)	D_e (eV)	ω_e (cm^{-1})	β (a.u.$^{-1}$)	a	b
Be_2 (40 Ry)	LDA	4.46	0.60	383.5	0.754	0.424	0.047
	LM	4.63	0.44	350.1	0.812	0.761	0.216
	BP	4.55	0.39	350.6	0.854	0.623	0.140
	Expt.	4.66	0.11	223.4			
Mg_2 (34 Ry)	LDA	6.30	0.24	124.0	0.619	0.452	0.067
	LM	6.55	0.14	113.4	0.738	0.357	0.131
	BP	6.73	0.09	89.0	0.740	0.288	0.076
	Expt.	7.35	0.05	51.1			
Ca_2 (24 Ry)	LDA	7.67	0.28	88.5	0.539	−0.111	0.129
	LM	8.07	0.17	72.0	0.563	0.533	−0.017
	BP	8.08	0.13	72.2	0.638	0.594	0.251
	Expt.	8.08	0.13	64.9			
Sr_2 (20 Ry)	LDA	8.20	0.27	55.3	0.505	1.926	0.098
	LM	8.46	0.22	51.6	0.529	1.342	0.305
	BP	8.51	0.15	47.6	0.589	0.997	0.288
Ba_2 (20 Ry)	LDA	8.52	0.39	48.9	0.466	1.044	0.175
	LM	8.67	0.33	45.4	0.468	1.108	0.345
	BP	8.59	0.29	46.4	0.517	0.823	0.319

Though not negligible, this is a small fraction of the total number of Fourier transforms required by a large supercell computation. For instance, the *ab initio* molecular dynamics (MD) has reached the size of about 100 atoms and 400 electrons per unit cell,[50] thus requiring, already at the LDA level, about 400 Fourier transforms per time step. The modifications to the LDA computer code are minor, both in two and three dimensions, and are restricted to the routines computing the XC energy and potential. In particular, this change does not affect directly the computation of the Hellmann-Feynman forces on the ions, which represent the delicate part of the *ab initio* MD program.

The potential-energy curves $V(r)$ computed in LDA, LM, and BP approximations have been fitted with the modified Morse potential of Hulburt and Hirshfelder,[51]

$$V(r)=D_e[(1-e^{-\beta x})^2+b\beta^3x^3e^{-2\beta x}(1+a\beta x)-1]\ , \quad (22)$$

where $x=r-r_e$ and r_e and D_e are the equilibrium distance and bonding energy, respectively. More so than in the LDA case, the fitting is required for the GC schemes to compute bonding parameters unaffected by small oscillations in the potential-energy curves. Part of these irregularities is due to the increased numerical noise implied by the higher kinetic-energy cutoff. Another part, in-

TABLE VII. Bonding parameters for the homonuclear dimers of the IIB elements computed in LDA and in the GC schemes. r_e, D_e, ω_e, a, and b are as in Table VI. The LDA results are from Ref. 6.

Dimer (E_{cutoff})		r_e (a.u.)	D_e (eV)	ω_e (cm^{-1})	β (a.u.$^{-1}$)	a	b
Cd_2 (109 Ry)	LDA	5.77	0.24	67	0.742	0.207	−0.098
	LM	6.03	0.08	39.8	0.782	−1.574	−0.457
	BP	6.54	0.04	36.0	1.189	0.451	0.289
	Expt.	9.10	0.05				
Hg_2 (80 Ry)	LDA	5.65	0.23	71	1.069	0.488	0.263
	LM	6.12	0.05	32.1	1.011	−1.774	−0.126
	BP	6.86	0.01	13.4	1.151	0.352	0.176
	Expt.	6.86	0.07				

stead, is a real feature of the GC schemes, and it is due to the oscillations of the XC potential and energy in the tail of the density distribution. Although the absolute magnitude of these effects is very small, their relative importance is enhanced by the flatness of $V(r)$ for these systems. The computed bonding parameters are collected in Tables VI (IIA elements) and VII (IIB elements), where they are compared to the available experimental data.

Before discussing the GC results, we mention that our data reveal an overestimate by LDA of the bonding in the IIA dimers even more severe than that reported in previous studies. In particular, we systematically obtain larger cohesive energies and shorter equilibrium distances than those of Ref. 5. This discrepancy, analogous to that found in Ref. 6 for the IIB dimers, is consistent with the improved completeness of the basis set used in the present computation.

For the IIA dimers the average LDA error with respect to the available experimental data is 7.9% for the equilibrium distance and 84% for the vibrational frequency. The cohesive energy is strongly overestimated, sometimes by a factor of 5. As reported in Ref. 6, the discrepancy is even larger for the IIB dimers.

The gradient-corrected schemes systematically improve over these results. Both the LM and the BP recipes significantly reduce the difference between computed and measured values for the cohesive energy, equilibrium distance, and vibrational frequency. Clearly, the quantitative agreement is still far from satisfactory, but it is also apparent that gradient corrections represent a big step in the right direction.

The best general description for the ground-state properties of these systems is provided by the BP formula. This finding, together with the trends discussed above for the pseudopotential smoothness and transferability, points to BP as the most promising scheme for performing improved total-energy computations at a minimal cost.

As expected, the improvement of the total energy does not correspond to an improved description of the electron density of states, as computed from the KS eigenvalues $\{\varepsilon_i\}$. In fact, the eigenvalues for both the occupied and unoccupied molecular orbitals are remarkably similar in LDA and in the LM or BP recipes. In all these schemes, the molecular bonding is related to the bending downwards of the $\{\varepsilon_i\}$ for the occupied states, indicating a covalent character for the cohesion of these molecules (see Refs. 4 and 47 for a discussion).

As a final remark, we mention that we performed computations for Mg_2 using the LDA pseudopotentials from the table of Ref. 45 and applying the GC to the valence charge only. This mixed scheme strongly reduced the improvement in the computed bonding parameters, thus confirming the importance of a consistent description of core and valence states via an "XC-dependent" pseudopotential.

VI. CONCLUSIONS

Gradient-corrected exchange-correlation functionals have been used in all-electron semirelativistic computa-

TABLE VIII. BP pseudopotential coefficients for the IIA elements. r_l^c, c_i, α_i, A_i, and B_i are defined in Appendix B.

Be $Z_v=2$ $r_1^c=0.4824$ $c_1=-1.091\,16$ $r_2^c=0.5881$ $c_2=2.091\,16$

l	i	α_i	A_i	B_i
0	1	2.0511	−22 700.705 52	18 199.267 91
	2	1.8083	−44 556.679 97	3172.231 63
	3	2.3001	67 260.110 95	6197.363 28
1	1	1.2621	−5 003.105 89	115.662 86
	2	1.4317	−35 207.079 58	3910.434 03
	3	1.5738	40 210.633 74	2537.340 51

Mg $Z_v=2$ $r_1^c=0.8237$ $c_1=-18.172\,48$ $r_2^c=1.2181$ $c_2=19.172\,48$

l	i	α_i	A_i	B_i
0	1	1.3714	26 539.894 25	−1820.072 13
	2	1.5603	−20 560.908 48	−4621.565 46
	3	1.9102	−5992.950 13	−674.950 01
1	1	1.0774	5138.082 81	−253.793 73
	2	1.1957	−5097.695 48	−386.978 64
	3	2.0860	−55.526 64	−18.604 04
2	1	1.1674	13 029.914 84	−760.178 99
	2	1.3776	30 465.721 05	−6358.952 36
	3	1.5428	−43 511.607 70	−2815.359 15

Ca $Z_v=2$ $r_1^c=0.4772$ $c_1=0.744\,88$ $r_2^c=2.3757$ $c_2=0.255\,12$

l	i	α_i	A_i	B_i
0	1	0.7136	3697.430 61	−144.255 12
	2	0.8162	−3489.515 82	−283.907 12
	3	1.2169	−203.501 43	−33.902 17
1	1	0.8074	−27 309.468 25	−7581.500 86
	2	0.7237	71 640.546 16	−1881.922 51
	3	0.9301	−44 327.215 52	−1975.870 36
2	1	3.7606	50 977.270 82	−11 329.678 41
	2	1.1059	23.110 99	−11.594 51
	3	4.2359	−51 004.333 61	−13 190.733 84

Sr $Z_v=2$ $r_1^c=0.5509$ $c_1=-28.677\,30$ $r_2^c=0.8694$ $c_2=29.677\,30$

l	i	α_i	A_i	B_i
0	1	1.1906	−73 197.029 16	3618.152 91
	2	1.3217	66 349.089 69	7671.205 90
	3	1.7044	6808.445 30	956.092 82
1	1	0.6370	−9222.931 64	267.703 64
	2	0.7006	9211.282 81	328.200 25
	3	2.2106	−28.776 12	13.049 57
2	1	0.7272	−33 206.067 34	1473.666 21
	2	1.1930	8041.985 71	1107.518 66
	3	0.8629	25 122.715 21	4633.757 46

Ba $Z_v=2$ $r_1^c=1.6136$ $c_1=-6.286\,82$ $r_2^c=0.7381$ $c_2=7.286\,82$

l	i	α_i	A_i	B_i
0	1	0.6264	12.243 60	−5.861 36
	2	0.3883	20.035 43	−1.160 13
	3	0.9674	−17.754 72	−7.489 15
1	1	0.5283	1309.887 84	−142.429 60
	2	0.6702	−1514.137 12	−106.496 81
	3	0.3618	217.303 32	−6.851 99
2	1	0.3741	7371.396 04	−172.618 98
	2	0.4640	11 534.310 99	−1481.278 27
	3	0.5536	−18 893.967 43	−709.015 14

tions for the atoms of the IIA and IIB elements. Our results confirm that, up to the heaviest elements, gradient corrections provide a systematic improvement over LDA for what concerns total energies, excitation, and ionization potentials.

For all these elements (with the exception of Zn) we have generated *ab initio* norm-conserving pseudopotentials to be used with the gradient-corrected functionals.

An extensive set of computations has been performed to assess the quality of these potentials. While the Perdew-Wang[18,19] functional is apparently unable to provide good pseudopotentials, we show that both the Langreth-Mehl[15] and Becke-Perdew[19,21] schemes give origin to pseudopotentials with the desirable properties of accuracy, smoothness, and transferability. A careful comparison shows that the BP scheme gives slightly better results than the LM functional.

These two sets of pseudopotentials have been used to compute bonding properties for the IIA and IIB homonuclear dimers. Again, our results show that both schemes provide an important and systematic improvement over LDA, with the BP scheme having an advantage with respect to the LM functional.

These findings point to the BP formula as the most promising candidate to replace the LDA in the determination of Born-Oppenheimer properties like total energies, equilibrium geometries, vibrational frequencies, and interatomic forces. The improvement in the computed properties can be very significant, especially for highly inhomogeneous systems like small aggregates (molecules and clusters) or surfaces. The inclusion of the BP gradient corrections in computer codes based on the plane-wave expansion is easy to implement and not very demanding in terms of CPU time.

Work is in progress along two different lines: (a) to include the BP functional in an *ab initio* molecular dynamics (Car-Parrinello) program, in order to study small clusters of the IIA elements, and (b) to evaluate the importance of gradient corrections in the computation of linear response functions for both finite systems and extended solids.

TABLE IX. BP pseudopotential coefficients for the IIB elements. r_i^c, c_i, α_i, A_i, and B_i are defined in Appendix B.

		Cd $Z_v=12$ $r_1^c=0.4477$ $c_1=1.871\,91$ $r_2^c=0.8448$ $c_2=-0.871\,91$		
l	i	α_i	A_i	B_i
0	1	1.3100	4824.280 50	473.330 01
	2	1.1687	−4864.534 35	262.450 95
	3	2.2005	77.187 56	−13.331 32
1	1	1.3793	3076.770 92	−273.971 64
	2	1.7315	7341.814 36	−2627.569 57
	3	2.0322	−10 384.963 68	−1325.358 00
2	1	8.5783	−59 905.274 79	35 247.400 43
	2	13.1010	41 639.732 06	40 708.433 13
	3	10.4545	18 295.022 98	146 885.355 03
		Hg $Z_v=12$ $r_1^c=0.4761$ $c_1=0.355\,92$ $r_2^c=0.7466$ $c_2=0.644\,08$		
l	i	α_i	A_i	B_i
0	1	1.1752	−6728.250 19	−2910.846 05
	2	1.0246	15 015.759 58	−685.200 75
	3	1.4423	−8267.092 81	−877.927 46
1	1	0.8744	6179.598 84	462.889 39
	2	0.7838	−6527.203 15	214.486 91
	3	1.2196	361.233 04	33.545 31
2	1	3.3287	−51 314.771 42	9650.211 88
	2	2.3610	−626.160 32	88.705 82
	3	3.6694	51 956.624 03	8563.555 10

ACKNOWLEDGMENTS

We thank G. B. Bachelet for sending us a copy of Ref. 25 prior to publication. This work has been supported by the Swiss National Science Foundation under Grant No. 20-5446.87 (G.O.) and No. 20-26535.89 (P.B.).

APPENDIX A: THE EXCHANGE POTENTIAL FOR THE BECKE APPROXIMATION

The exchange-potential corresponding to the Becke approximation [Eqs. (10) and (11) of Sec. II] is computed from the standard expression of variational calculus:

$$\frac{\delta E_X^B}{\delta\rho_\sigma(\mathbf{r})}=\mu_x^{\mathrm{LSD}}+\frac{\partial f}{\partial\rho_\sigma}-\sum_{i=1}^{3}\frac{d}{dx_i}\left[\frac{\partial f}{\partial(d\rho_\sigma/dx_i)}\right], \tag{A1}$$

where μ_x^{LSD} is the LSD exchange potential.

This gives

$$\frac{\delta E_X^B}{\delta\rho_\sigma(\mathbf{r})}=\mu_x^{\mathrm{LSD}}-\frac{\beta}{G_\sigma^2}\left[\tfrac{4}{3}\rho_\sigma^{1/3}x_\sigma^2G_\sigma-2[1+3\beta x_\sigma(y_\sigma-x_\sigma F_\sigma)]\frac{\nabla^2\rho_\sigma}{\rho_\sigma^{4/3}}+6\beta\rho_\sigma^{1/3}\left[\frac{\nabla\rho_\sigma\cdot\nabla|\nabla\rho_\sigma|}{\rho_\sigma^3}-\tfrac{4}{3}x_\sigma^3\right]\right.$$
$$\left.\times\left[x_\sigma F_\sigma^3+\frac{3y_\sigma(1+2\beta x_\sigma y_\sigma)+4x_\sigma F_\sigma(1-3\beta x_\sigma^2F_\sigma)}{G_\sigma}\right]\right], \tag{A2}$$

where

$$x_\sigma=\frac{|\nabla\rho_\sigma|}{\rho_\sigma^{4/3}},$$

$$y_\sigma=\sinh^{-1}x_\sigma,$$

$$G_\sigma=1+6\beta x_\sigma y_\sigma,$$

and

$$F_\sigma=\frac{1}{\sqrt{1+x_\sigma^2}}.$$

APPENDIX B: THE BECKE-PERDEW PSEUDOPOTENTIALS

The LM and BP pseudopotentials, computed numerically on a logarithmic mesh, have been fitted to the analytic form introduced in Ref. 45:

$$V_l(r) = -\frac{Zv}{r}\sum_{i=1}^{2} c_i \mathrm{erf}(r/r_i^c) + \sum_{i=1}^{3} (A_i^l + r^2 B_i^l) e^{-\alpha_i r^2},$$

where l is the angular moment.

The coefficients c_i, r_i^c, α_j, A_j^l, and B_j^l for the BP pseudopotentials are reported in Table VIII (IIA elements) and Table IX (IIB elements). This analytic form suffers from the well-known problems due to the extreme non-linearity of the fit, as discussed, for instance, in Ref. 52. These problems, however, do not have important practical consequences, apart from the need to report in the tables and to use in the computations a large number of digits for the A_j^l and B_j^l coefficients. The fitting coefficient for the LM scheme, together with the numerical pseudopotentials for both BP and LM, are available on request.

[1]P. Hohenberg and W. Kohn, Phys. Rev. **136**, B864 (1964).
[2]W. Kohn and L. J. Sham, Phys. Rev. **140**, A1133 (1965).
[3]G. P. Srivastava and D. Weaire, Adv. Phys. **36**, 463 (1987).
[4]R. O. Jones and O. Gunnarsson, Rev. Mod. Phys. **61**, 689 (1989).
[5]R. O. Jones, J. Chem. Phys. **71**, 1300 (1979).
[6]P. Ballone and G. Galli, Phys. Rev. B **42**, 1112 (1990).
[7]R. Car and M. Parrinello, Phys. Rev. Lett. **55**, 2471 (1985).
[8]R. G. Parr and W. Yang, *Density Functional Theory of Atoms and Molecules* (Oxford University Press, Oxford, 1989).
[9]J. P. Perdew and A. Zunger, Phys. Rev. B **23**, 5048 (1981); I. Lindgren, Int. J. Quantum Chem. **5**, 411 (1971).
[10](a) O. Gunnarsson and B. I. Lundqvist, Phys. Rev. B **13**, 4274 (1976); (b) O. Gunnarsson, M. Jonson, and B. I. Lundqvist, *ibid.* **20**, 3136 (1979).
[11]O. Gunnarsson, M. Jonson, and B. I. Lundqvist, Phys. Lett. **59A**, 177 (1976); Solid State Commun. **24**, 765 (1977); see also Ref. 10(b).
[12]J. A. Alonso and L. A. Girifalco, Solid State Commun. **24**, 135 (1977).
[13]O. Gunnarsson and R. O. Jones, Phys. Scr. **21**, 294 (1980).
[14]D. C. Langreth and J. P. Perdew, Phys. Rev. B **15**, 2884 (1977); **21**, 5469 (1980).
[15]D. C. Langreth and M. J. Mehl, Phys. Rev. Lett. **47**, 446 (1981).
[16]D. C. Langreth and M. J. Mehl, Phys. Rev. B **28**, 1809 (1983); **29**, 2310(E) (1984).
[17](a) C. D. Hu and D. C. Langreth, Phys. Scr. **32**, 391 (1985). Equation (2.26) for the XC potential contains some errors. (b) See F. W. Kutzler and G. S. Painter, Phys. Rev. B **37**, 2850 (1988) for a corrected formula.
[18]J. P. Perdew and Wang Yue, Phys. Rev. B **33**, 8800 (1986).
[19]J. P. Perdew, Phys. Rev. B **33**, 8822 (1986).
[20]A. D. Becke, J. Chem. Phys. **84**, 4524 (1986); **85**, 7184 (1986).
[21]A. D. Becke, Phys. Rev. A **38**, 3098 (1988).
[22]U. von Barth and R. Car (unpublished).
[23]M. R. Norman and J. P. Perdew, Phys. Rev. B **28**, 2135 (1983); M. Norman and D. D. Koelling, *ibid.* **28**, 4357 (1983).
[24]K. Schönhammer and O. Gunnarsson, Phys. Rev. B **37**, 3128 (1988); D. Mearns and W. Kohn, *ibid.* **39**, 10669 (1989).
[25]E. L. Shirley, R. M. Martin, G. B. Bachelet, and D. M. Ceperley, Phys. Rev. B **42**, 5057 (1990).
[26]F. Herman, J. P. Van Dyke, and I. B. Ortenburger, Phys. Rev. Lett. **22**, 807 (1969).
[27]K. H. Lau and W. Kohn, J. Phys. Chem. Solids **37**, 99 (1976).
[28]J. P. Perdew, D. C. Langreth, and V. Sahni, Phys. Rev. Lett. **38**, 1030 (1977).
[29]D. M. Ceperley, Phys. Rev. **18**, 3126 (1978); D. M. Ceperley and B. J. Alder, *ibid.* **45**, 566 (1980).
[30]C. D. Hu and D. C. Langreth, Phys. Rev. B **33**, 943 (1986).
[31]M. Rasolt and D. J. W. Geldart, Phys. Rev. **13**, 1477 (1976).
[32]C.-O. Almbladh and U. von Barth, Phys. Rev. B **31**, 3231 (1985).
[33]See the original papers and A. C. Pedroza, Phys. Rev. B **33**, 804 (1986); F. W. Kutzler and G. S. Painter, Phys. Rev. Lett. **59**, 1285 (1987); J. B. Lagowski and S. H. Vosko, J. Phys. B **21**, 203 (1988).
[34]A. Savin, U. Wedig, H. Preuss, and H. Stoll, Phys. Rev. Lett. **53**, 2087 (1984); A. D. Becke, Ref. 20; F. W. Kutzler and G. S. Painter, Ref. 17(b).
[35]See Refs. 23 and 22; U. von Barth and A. C. Pedroza, Phys. Scr. **32**, 353 (1985); P. Bagno, O. Jepsen, and O. Gunnarsson, Phys. Rev. B **40**, 1997 (1989); B. Barbiellini, E. G. Moroni, and T. Jarlborg, J. Phys. Condens. Matter **2**, 7597 (1990).
[36]Z. Y. Zhang, D. C. Langreth, and J. P. Perdew, Phys. Rev. B **41**, 5674 (1990).
[37]S. H. Vosko, L. Wilk, and M. Nusair, Can. J. Phys. **58**, 1200 (1980).
[38]C. E. Moore, *Atomic Energy Levels,* Publ. No. NSRDS-NBS 34, Natl. Bur. Stand. Ref. Data Ser., Natl. Bur. Stand. (U.S.) (U.S. GPO, Washington, D.C., 1970).
[39]J. Malý and M. Hussonnois, Theor. Chim. Acta **28**, 363 (1973).
[40]U. von Barth, Phys. Rev. A **20**, 1693 (1979).
[41]J. P. Perdew, in *Density Functional Theory,* edited by J. Keller and L. J. Gázquez (Springer, Berlin, 1983), p. 127.
[42]For some of the elements the very small value of E^{SI} computed in GC schemes is partly due to cancellation of contributions coming from different orbitals. However, summing the absolute value of the orbital contributions does not change the conclusion that GC schemes greatly reduce E^{SI}.
[43]D. R. Hamann, Phys. Rev. B **40**, 2980 (1989).
[44]All the pseudopotentials, including the LDA one, have been generated with the same parameters.
[45]G. B. Bachelet, D. R. Hamann, and M. Schlüter, Phys. Rev. B **26**, 4199 (1982).
[46]S. G. Louie, S. Froyen, and M. L. Cohen, Phys. Rev. B **26**, 1738 (1982).
[47]Preliminary results have been presented at a conference and they will be published in Z. Phys. D.
[48]S. N. Khanna, F. Reuse, and J. Buttet, Phys. Rev. Lett. **61**, 535 (1988); F. Reuse, S. N. Khanna, V. de Coulon, and J. Buttet, Phys. Rev. B **41**, 11743 (1990); R. Kawai and J. H. Weare, Phys. Rev. Lett. **65**, 80 (1990).
[49]K. Rademann, B. Kaiser, U. Even, and F. Hensel, Phys. Rev. Lett. **59**, 2319 (1987); C. Brechignac, M. Broyer, P. Cahuzac, G. Delacretaz, P. Labastie, J. P. Wolf, and L. Woste, *ibid.* **60**, 275 (1988).
[50]F. Buda, G. L. Chiarotti, R. Car, and M. Parrinello, Phys. Rev. Lett. **63**, 294 (1989).
[51]H. M. Hulburt and J. O. Hirschfelder, J. Chem. Phys. **9**, 61 (1941); **35**, 1901 (1961); see also A. C. Hurley, *Introduction to the Electron Theory of Small Molecules* (Academic, London, 1976), p. 8, for a discussion.
[52]W. E. Pickett, Comput. Phys. Rep. **9**, 115 (1989).